Research on calibration method in lab of direct solar channels of Sun photometer

Maopeng Xia (夏茂鹏)[1], Jianjun Li (李健军)[1], Zhengqiang Li (李正强)[2], Dongyang Gao (高冬阳)[1], Weiwei Pang (庞伟伟)[1], Donghui Li (李东辉)[2], and Xiaobing Zheng (郑小兵)[1*]

[1]*Key Laboratory of Optical Calibration and Characterization, Chinese Academy of Sciences, Hefei 230031, China*

[2]*Institute of Remote Sensing Applications, Chinese Academy of Science, Beijing 100101, China*

[*]*Corresponding author: xbzheng@aiofm.ac.cn*

Received June 27, 2014; accepted October 11, 2014; posted online November 28, 2014

We develop a new calibration method in lab by measuring the absolute spectral irradiance responsivity of Sun photometer sun channel. The absolute power responsivity of Sun photometer is obtained when a white laser double monochromator system serve as a source, and a standard transfer detector calibrated against cryogenic absolute radiometer is assembled to measure the absolute power of laser beam. The effective area of aperture is measured through laser raster scanning method, and the relative spectral irradiance responsivity of the corresponding channel is obtained by using tungsten–halogen lamps double monochromator system. On the basis of the above results, the top of the atmosphere responsive constants V_0 (500, 675, and 870 nm) are obtained by integration with extraterrestrial solar spectral irradiance data. Comparing the calibration results with that of CIMEL, France in November 2011, the relative differences are 4.38%, 2.23%, and 2.45%, respectively. The calibration uncertainty reaches to 2.048×10^{-2}, which shows a remarkable consistency with the Langley plot method. Further, our scheme can overcome the limits of space and atmospheric conditions which are only available at a high-altitude calibration site in particular date. The advantages lie in not only shortening the experiment period but also being of high precision. This new scheme definitely plays an important role in supporting the current and future sun photometry calibration activities which are significant to earth observation.

OCIS codes: 120.0120, 120.028, 120.3930.

doi: 10.3788/COL201412.121201.

Ground-based Sun photometer was designed to measure direct solar irradiance and diffused sky radiance at different wavelengths. Currently, it serves as a standard radiometric instrument in the spectral characteristics of solar radiation. Sun photometer is also significant with regard to the passive remote sensing of aerosols including the aerosol optical thickness, phase function, single scattering reflectance, particle number distribution, and other parameters which can be used to evaluate the current aerosol model.

Nowadays, the aerosol automatic observation network[1,2] consists of about 400 automatic Sun photometers, which have already provided vast quantities of aerosol and microphysical parameters data, water vapor content, cloud radiation, and other atmospheric information of high quality for the research on atmospheric climate change, validation of satellite remote sensing, environmental monitoring, and other fields.

The V_0 coefficient of Sun photometer direct channel is traceable to the calibration result at high-altitude coordinates. Generally, the calibration is carried out on high mountains by the Langley plot measurement to obtain V_0 coefficient of the instrument[3,4] under desired atmospheric conditions, during which solar serves as a reference source. The basic principle of the Langley plot method is shown as follows.

According to Beer–Lambert–Bouger attenuation law, the output voltage $V_s(\lambda)$ of Sun photometer can be obtained when the direct solar irradiance is observed over each channel.

$$V_s(\lambda) = V_0(\lambda)R^{-2}\exp[-\tau(\lambda)m(\theta)], \tag{1}$$

where $\tau(\lambda)$ is the total spectral optical depth, $V_0(\lambda)$ is the instrument calibration constant, R is the Earth–Sun distance in astronomical units at the time of observation, and m is the relative optical air mass which is a function of solar zenith angle θ.

Taking the logarithm of Eq. (1) leads to

$$\ln V_s(\lambda) = \ln V_0(\lambda) - 2\ln R - m(\theta)\tau(\lambda), \tag{2}$$

$\tau(\lambda)$ is set as a constant during $m(\theta)$ ranges. We can take a series of measurements. Thus, $V_0(\lambda)$ can be obtained by taking antilogarithmic of vertical intercept by fitting $V_s(\lambda)$ versus $m(\theta)$ through a least-squares method. During the short-period calibration process, the value of R can be considered as a constant.

The V_0 coefficient of Sun photometer can be calibrated via a master Sun photometer using cross-calibration technique with combined standard uncertainty of 0.5%–1.0%. In fact, only master instruments are calibrated on high mountains on a frequent basis, the others are generally calibrated by comparison with the

master instrument at low altitude which is expensive and time-consuming. The accuracy of this method will be reduced with the transfer chain getting longer. Especially, no similar high-altitude point calibration site is qualified in China, which makes it difficult to satisfy the requirements of a dynamic observation if the instrument is traceable to foreign master instrument. For the above reasons, it is urgently necessary to develop a new lab calibration method to replace the current method. It is also an important direction of development expected to improve the calibration accuracy in the meantime.

The Sun photometer is required to be calibrated regularly. Both China and foreign countries have carried much work in terms of Sun photometer. Schmid *et al.* performed repeated calibrations of Sun photometer by means of irradiance standard lamps and their results showed a deviation of 4.9% for the different channels compared with the Langley plot[5]. Campanelli *et al.* made use of a modified version of the Langley plot based on an inversion code of column-integrated aerosol size distribution. The precision of the method was estimated to within 1%–2.5% depending on the wavelength[6]. Li *et al.* introduced a gain-corrected solid angle method and the results showed that the uncertainty of vicarious radiance calibration was 3%–5% compared with lab calibration[2]. Chen *et al.* calibrated multi-filter rotating shadow-band radiometer by Angstrom's law, which linked aerosol optical depth (AOD) at multiple wavelengths as the primary constraint and also used the bi-channel Langley regression to provide an additional constraint. Chen *et al.* showed that the upper limit of the error of 870 channels final V_{0S} is less than 1.03%[7].

Based on the integrating sphere which was traced from the National Institute of Standard and Technology method, Tao *et al.* calibrated CE318 Sun photometer[8]. It was shown that the instrument coefficients differed by less than 3% for visible (~5% for infrared) wavelengths from the original ones stated by CIMEL Electronique[8]. It uses the Angstrom law that links AOD at multiple wavelengths as the primary constraint. It also uses the bi-channel Langley regression to provide an additional constraint.

The research on Sun photometer laboratory calibration method was first established by our groups in China. A tunable laser based on integrating sphere is used to calibrate diffused sky channel of Sun photometer[9]. A tunable laser into integrating method was applied to calibrate the direct channel of Sun photometer[10]. During the procedure, signal-to-noise ratio (SNR) of the measurement result was low due to the weak irradiance which was about two magnitudes less than the Sun irradiance. In addition, it was subject to the disturbance of laser speckle on detecting plane and measurement of distance between aperture stop and the exit of integrating sphere. With the limitations of the geometric error and fitting methods, experimental results were not satisfied. The absolute irradiance responsivity of Sun photometer sun channel (870 nm) was obtained by using raster scanning of a single collimated laser beam to generate the uniform irradiance field[11]. This method has two advantages with high laser power and high SNR. However, several shortcomings limit its applications, such as the complex tuning of laser wavelength, long-period single channel scanning, and requirement of stability of source.

In this letter, we report a new method dealing with the calibration of Sun photometer solar direct channels. The new system, named white laser-based facility, consists of a white laser (Fig. 1) and double monochromator– has several advantages, such as high output laser power, easy wavelength tuning, short-period calibration process for single channel, and high precision. Compared with the white laser consumption, the Langley plot method will spend more in the long term and our client's attention are focused on the short-period calibration. It is more suitable for Sun photometer regular calibration under lab conditions.

The absolute power responsivity of Sun photometer (500, 675, and 870 nm) is obtained when the white laser-based facility is served as a source and a standard transfer detector calibrated against cryogenic absolute radiometer is used to measure the absolute power of laser beam. The effective area of aperture is determined by the laser raster scanning method[12–14]. The relative spectral irradiance responsivity of the corresponding channel is obtained by using tungsten–halogen lamps and double monochromator system. On the basis of the above results, the top of the atmosphere responsive V_0 coefficient (500, 675, and 870 nm) can be obtained by integration with extraterrestrial solar spectral irradiance data.

To determine the calibration coefficient V_0 of Sun photometer, component-based calibration was adopted. The flow of data processing is shown in Fig. 2. The Sun photometer absolute spectral responsivity of a specifically wavelength was the product of absolute power responsivity and effective area of aperture. The former could be obtained by using a standard transfer detector calibrated against cryogenic to measure the absolute power of laser which was sourced by a white

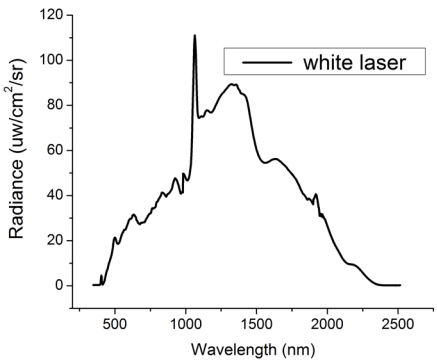

Fig. 1. Radiance of white laser.

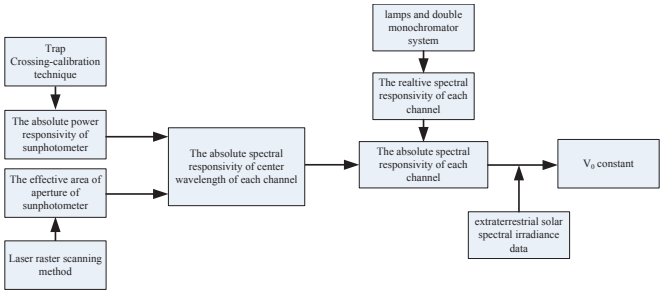

Fig. 2. Schematic diagram of Sun photometer calibration.

laser double monochromator system, and the latter was measured through laser raster scanning method. The relative spectral responsivity of each channel was acquired by using tungsten–halogen lamps double monochromator system. On the basis of above results, we attained the absolute spectral responsivity of a channel. The top of atmosphere responsive constant V_0 was then calculated by combining the extraterrestrial solar spectral irradiance data.

The white laser double monochromator system generated a narrow-band Gaussian beam. The output beam of double monochromator which passed through a spatial filter was much smaller than the Sun photometer aperture area. A relative throughput of 0.9999 requires that the ratio of the aperture and the beam diameters meet

$$\frac{D}{d_{\mathrm{L}}} >> 2.15, \tag{3}$$

where D is the diameter of the effective aperture stop and d_{L} is the diameter of laser beam. The uniform irradiance field E_1 can be represented as

$$E_1 = \frac{P_{\mathrm{L}}}{S_0}, \tag{4}$$

where S_0 is the area of the laser beam and P_{L} is the power of the laser beam. The output generated by the instrument is expressed as digital number (DN) DN_1. Assuming the aperture of Sun photometer is filled with the equivalent uniform light field, the output of Sun photometer turns into DN_z. The relationship between DN_1 and DN_z is

$$\mathrm{DN}_z = \mathrm{DN}_1 \frac{S_{\mathrm{p}}}{S_0}, \tag{5}$$

where S_{p} is the aperture area of Sun photometer. According to the definition of the absolute spectral irradiance responsivity, the Sun photometer absolute irradiance responsivity $R_{\mathrm{E}}(\lambda)$ at a given wavelength can be summarized as

$$R_{\mathrm{E}}(\lambda) = \frac{\mathrm{DN}_z}{E_1} = \frac{\mathrm{DN}_1 \dfrac{S_{\mathrm{p}}}{S_0}}{\dfrac{p_{\mathrm{L}}}{S_0}} = \frac{\mathrm{DN}_1}{P_{\mathrm{L}}} S_{\mathrm{p}}, \tag{6}$$

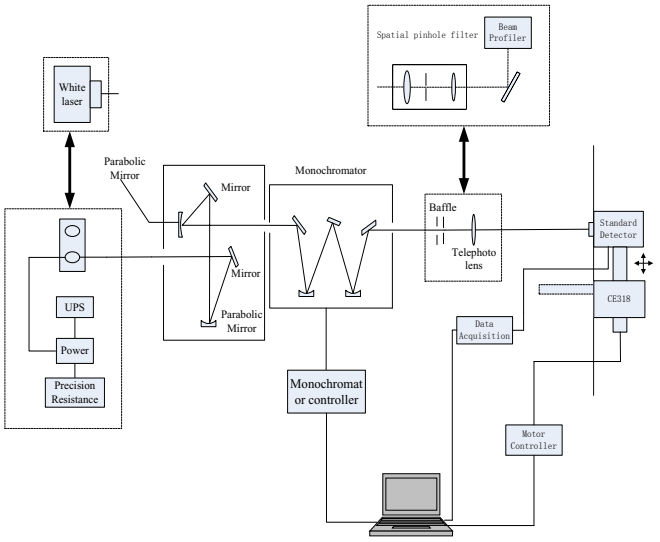

Fig. 3. Schematic diagram of absolute power irradiance responsivity calibration and relative spectral responsivity system.

where the value of DN_1 can be obtained by CE318, the laser power P_{L} can be measured by standard detector, and the effective area of aperture S_{p} is measured by laser raster scanning method.

Based on the above results, the absolute spectral responsivity of corresponding channel can be expressed as

$$R_{\mathrm{E}}(\lambda') = R_{\mathrm{E}}(\lambda) \frac{R_{\Phi}(\lambda')}{R_{\Phi}(\lambda)}, \tag{7}$$

where $R_{\Phi}(\lambda)$ and $R_{\Phi}(\lambda')$ represent the relative spectral responsivities at different wavelengths which can be acquired by using lamp monochromator system. The top of the atmosphere responsive V_0 coefficient obtained by integration with extraterrestrial solar spectral irradiance data is shown as

$$V_0 = \int_{\lambda_1}^{\lambda_2} R_{\mathrm{E}}(\lambda) E_{\mathrm{sun}}(\lambda)\,\mathrm{d}\lambda, \tag{8}$$

where $E_{\mathrm{sun}}(\lambda)$ is the extraterrestrial solar spectral irradiance data, λ_1 is the minimum wavelength, and λ_2 is the maximum wavelength of the channel.

CE318 designed by CIMEL Corporation is an automatic rotating filter sun–sky radiometer. It contains nine narrowband (10 nm full-width at half-maximum) interference filters centered from 340 to 1640 nm and the field of view is 1°.

The visible to near-infrared spectral comparator facility was a lamp-based system used to measure the relative spectral irradiance responsivity of Sun photometer (Fig. 3). The main component of the monochromator was a double prism grating and its entrance slit was illuminated by a 250 W tungsten-halogen lamp (HLX64655, OSRAM Corporation). The lamp was controlled by a high accuracy stable power. In order to converge rays better, an optic system (two-off axis

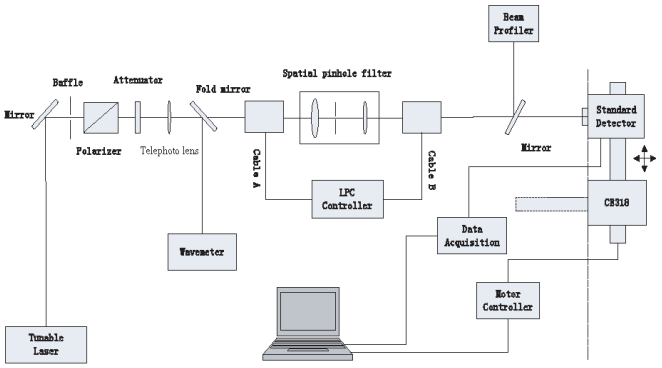

Fig. 4. High accuracy measurement of aperture-area system.

parabolic mirrors and two high reflection mirrors) was fixed in front of the monochromator. The typical exit slit was set to 1.0 mm. By controlling the dispersion of monochromator, a desired quasi-Lambertian source was provided. The bandwidth of the monochromator was 2 nm. A shutter was located just behind the exit slit which was used to measure background noise. After passing the monochromator, the beam crossed through two apertures, and then through a long-focus lens (300 mm lens) for imaging the aperture onto standard detectors or Sun photometer. The positions of standard detector and Sun photometer were adjusted by a pair of orthogonal linear precision translation stage. The Sun photometer standard detector, and exit optics were enclosed in a light-tight box. The output signals from standard detector were acquired by Agilent acquisition card.

The schematic diagram of the absolute power responsivity system is shown in Fig. 3. A white laser with high power (sc450-8, Fianinum Corporation) was introduced into a double monochromator, which could produce a quasi-Lambertian and high radiant flux source. Other processes were similar to the above. The output beam was sent into a spatial filter (a lens with a focus length of 38 mm and a diamond pin-hole, 100 μm of diameter) in order to eliminate the marginal rays and then it was collimated by a system of lenses to a diameter of d_{L} ~0.5 mm. Finally, the beam was received by the detector. The absolute power responsivity of Sun photometer could be achieved by using cross-measuring technique.

A schematic view of the area-aperture measurement is shown in Fig. 4. The tunable laser beam was first directed through a high reflection mirror, and then it was attenuated with a neutral density filter after which it was polarized. The intensity of this polarized beam was stabilized by laser power controller (LPC) which controls the relative optical to within 0.05% (8 h) of the set point. Finally, the laser beam was spatially filtered and collimated to standard detector. A beam splitter sent portion of laser beam into wavemeter (Bristol NIR) that measured the wavelength of the radiation within 0.001 nm. Sun photometer and standard detector were assembled on 2D precision translation stage. The aperture-area measurement was obtained by moving the Sun photometer and standard detector with a high accuracy translation stage step by step relative to the laser beam.

A spatially uniform irradiance was formed over the aperture by overlapping identical, parallel laser beams centered at the aperture stop of Sun photometer in an orthogonal lattice. The ratio of the throughout power and irradiance gave the area of aperture. Beam profiler was used to measure the incident laser diameter.

The absolute power responsivity (Fig. 5) of the standard detector from 350 to 1064 nm was calibrated by cryogenic radiometer. Uncertainties of cryogenic radiometer and standard detectors at seven wavelengths in the visible spectrum (488–786 nm) were less than 0.023% and 0.035%, respectively[15]. In the visible (412–800 nm) region, the total relative standard uncertainty of the spectral responsivity was less than 0.05%, whereas in the ultra-violet (350 nm) and near-infrared regions above 800 nm, the total relative standard uncertainty for both was less than 0.065%[16]. The responsivity in the wavelength ranging from 490 to 510, 665 to 685, and 860 to 880 nm was obtained by an internal interpolation method.

According to tunable laser system, the aperture area of Sun photometer is shown in Table 1. The areas were 13.187 and 13.057 mm^2, respectively. The coefficient of variance was 4.954×10^{-3}, which is in good agreement with the report[17].

Three Sun photometer channels were calibrated in this work. Relative spectral responsivity of each channel (Fig. 4) was measured at a scanning step of 1 nm within ±10 nm of channel's center wavelength by using lamp monochromator-based facility. Measurements at 380 and 440 nm channels were not available because of the low lamp luminous.

The responsivity of Sun photometer at the edges of filter is extremely smooth and the data out of band is very small (Fig. 5, bold line). According to the manufacturer, the filter out of band contribution is generally less than 10^{-4} which can be neglected in this measurement.

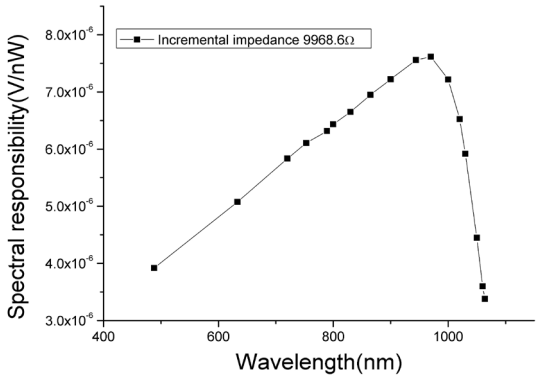

Fig. 5. Spectral power responsivity of the standard detector.

Table 1. Effective Aperture Area of Sun Photometer

Data	Area (mm^2)
January 13, 2014	13.187
January 8, 2014	13.057
Average	13.122

The relationship between the normalized relative spectral irradiance responsivity and the relative power responsivity profiles should be exactly identical. The lamp monochromatic-based facility provided a determination of the relative spectral responsivity of Sun photometer channels. The manufacturer-supplied filter transmittance might differ from the Sun photometer total spectral responsivity, which made it necessary to compare with filter transmission profiles in the calibration activity or in high precision data processing. In Fig. 6, the relative spectral irradiance responsivity of each channel is compared with filter transmittance profiles. It was apparent that all channels' center wavelength slightly shifted 0.5 nm to longer wavelength which was probably caused by the interaction with the filter when the incidence was not normal.

The effective aperture area of Sun photometer from the tunable laser facility is calculated by Eq. (6), and the area is 13.122 mm^2. The value of $R_E(\lambda)$ at different wavelengths (500, 675, and 870 nm) is estimated by inversion of Eq. (6), where S_p is calculated according to Eq. (5), P_L is measured by standard detector, and DN_1 is directly accessed from the Sun photometer. The absolute spectral responsivity of the channels can be obtained by combining the normalized relative irradiance responsivity with $R_E(\lambda)$ at different channels' center wavelengths. The profiles of each channel are shown in Fig. 7 (symbol line). Measurement at 1020 nm channel is not available temporally because the wavelength is near the peak length wavelength (1064 nm) of which the noise plays a dominant role[18].

Table 2. Responsive V_0 Coefficients of Sun Photometer and Relative Deviation

Channel (nm)	AIOFM	CIMEL (2011)	Relative Deviation (%)
500	24197	23181	4.38
675	25473	26053	2.23
870	20066	20570	2.4

On the basis of the above results, the top of the atmosphere responsive V_0 coefficients of 500, 675, and 870 nm channels were obtained by integrating with extraterrestrial solar spectral irradiance data. The coefficients of the corresponding channels are presented in Table 2. Compared with the result provided by CIMEL which was acquired by using the traditional Langley plot method in 2011, the relative deviations were 4.38%, 2.23%, and 2.45%, respectively. The relative deviation at 500 nm was relatively larger which was perhaps due to lack of radiant flux from the source.

The dominant uncertainties in the calibration of V_0 coefficients of Sun photometer mainly originated from the combination of the uncertainties in the spectral power responsivity, the accuracy of solar spectral irradiance data, the calibration process, and the temperature sensitivity of Sun photometer. Berjón *et al.*[19] proved that for 1020 nm channel of Sun photometer CIMEL 318, the relative change in signal due to temperature was about 2.5×10^{-3} $℃^{-1}$ and for other channels, the dependency was significantly lower, and the uncertainty of the temperature coefficient was about 5.0×10^{-4} $℃^{-1}$ for the other channels. Assuming that each uncertainty component is independent, the uncertainty evaluation in accordance with international protocol of each component is presented in Table 3.

The uncertainty of absolute power responsivity of the trap is directly acquired by the calibration process against cryogenic radiometer. Multi-point interpolation

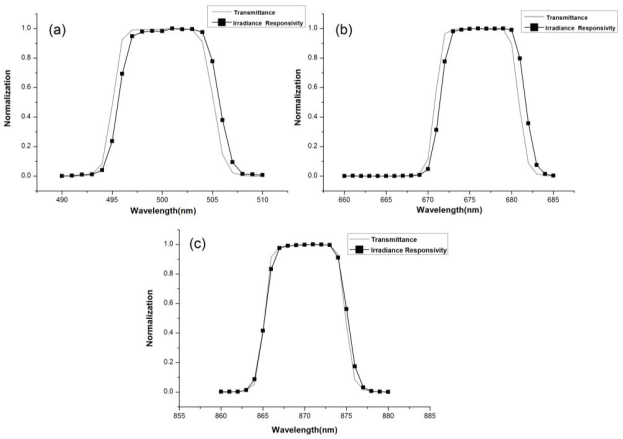

Fig. 6. Comparison of relative spectral irradiance responsivity and filter transmittance profile of CE318 Sun photometer: (a) 500, (b) 675, and (c) 870 nm.

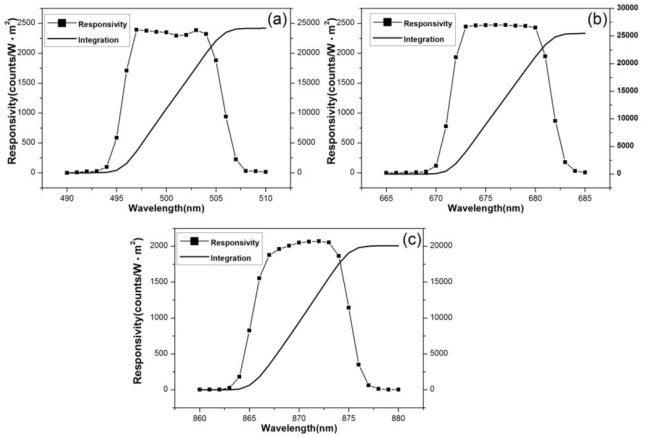

Fig. 7. Absolute spectral irradiance responsivity of Sun photometer and integration of responsivity and solar spectral irradiance: (a) 500, (b) 675, and (c) 870 nm

Table 3. Component of Uncertainty and their Contributions

Uncertainty Component		**Relative Standard Uncertainty**
Area Aperture	Trap Radiant Power Responsivity	4.15×10^{-4}
	Responsivity Interpolation	2.15×10^{-3}
	I-V Gain	1.76×10^{-3}
	Source Stability (75 min)	6.8×10^{-4}
	Planar Motion Nonuniformity	0.80×10^{-4}
Relative Spectral Responsivity	Lamp Instability	1.00×10^{-4}
	Monochromator's Repeatability	3.10×10^{-3}
	Source's Stability	1.00×10^{-4}
	Trap's Stability	1.00×10^{-4}
	Linear of Sun Photometer	3.18×10^{-4}
Absolute Spectral Responsivity	White Laser Stability (5 min)	1.10×10^{-3}
	Top-of-the-atmosphere Spectral	2.00×10^{-2}
	Planar Motion Nonuniformity	0.80×10^{-4}
	Trap's Stability	1.00×10^{-4}
	Linear of Sun Photometer	3.18×10^{-4}
Temperature Sensitivity		5.00×10^{-4}
Combined Uncertainties		2.048×10^{-2}

is applied to obtain absolute power responsivity of a corresponding wavelength, the value of the interpolation uncertainty is shown in Ref. [9].

A standard trap was exposed to source (lamp and laser beam) for 75 min, of which the uncertainty can be calculated by a method similar to the above. The uncertainties of linear precision translation stage, double monochromator, the spectral of the top of the atmosphere, and linear of Sun photometer are obtained against mercury lamp[10,20].

In conclusion, the scheme for absolute spectral radiance responsivity calibration involves a white laser serving as a source, double monochromator creating a high-intensity quasi-Lambertian, and standard detector which is traceable to cryogenic radiometer. The laser raster scanning method is adopted to measure the effective area of aperture and relative spectral irradiance responsivity of the corresponding channel by using tungsten–halogen lamps and double monochromator system. A Sun photometer-NE is calibrated by this process. Comparing the calibration results with that of CIMEL, the relative differences are 4.38%, 2.23%, and 2.45%, respectively. The calibration uncertainty reaches to 2.048×10^{-2}, which shows an equivalent uncertainty with the Langley plot method. The principle feasibility of this new method is validated. Improving the stability of white laser-based system and the accuracy of extraterrestrial solar irradiance data will be considered in future research. As the effective aperture area of Sun photometer remains unchangeable during the measuring process, other channels can be calibrated by using the above method.

The improved radiance responsivity calibration precision enables to gain more accurate aerosol property retrievals. Currently, about 100 Sun photometers in China lack trustable calibration facility. If the irradiance responsivity can be precisely measured based on a similar method, it can be a potential competitive approach to the traditional Langley plot method. Considering the limitations of the Langley plot method, such as high precision only available at a few tops of high mountains, our scheme can be extremely useful to support current and future Sun photometry calibration activities, which are significant components of earth observation system.

This work was supported by the National 973 Project Fund (No. 2010CB950801) and the National Natural Science Foundation of China (No. 61275173).

References

1. B. Holben, T. Eck, I. Slutsker, D. Tanre, J. Buis, A. Setzer, E. Vermote, J. Reagan, Y. Kaufman, and T. Nakajima, Remote Sens. Environ. **66,** 1 (1998).
2. Z. Li, L. Blarel, T. Podvin, P. Goloub, J. P. Buis, and J. P. Morel, Appl. Opt. **47,** 1368 (2008).
3. G. E. Shaw, J. A. Reagan, and B. M. Herman, J. Appl. Meteorol. **12,** 374 (1973).

4. X. Wang, Y. Qiao, P. Goloub, and Z. Li, Acta Opt. Sin. **28,** 87 (2008).
5. B. Schmid and C. Wehrli, Appl. Opt. **34,** 4500 (1995).
6. M. Campanelli, T. Nakajima, and B. Olivieri, Appl. Opt. **43,** 651 (2004).
7. M. Chen, J. Davis, H. Tang, Z. Gao, and W. Gao, Proc. SPIE **8513,** 851305 (2012).
8. R. Tao, H. Che, Q. Chen, Y. Wang, J. Sun, X. Zhang, S. Lu, J. Guo, H. Wang, and X. Zhang, Particuology **13,** 88 (2014).
9. Q. Xu, X. Zheng, W. Zhang, and X. Wang, Acta Opt. Sin. **30,** 1337 (2010).
10. W. Zhai, J. Li, X. Zheng, Z. Li, B. Meng, W. Zhang, and X. Wang, Acta Opt. Sin. **32,** 131 (2012).
11. W. Xu, J. Li, and X. Zheng, Spectrosc. Spectr. Anal. **33,** 255 (2013).
12. V. Ahtee, S. W. Brown, T. C. Larason, K. R. Lykke, E. Ikonen, and M. Noorma, Appl. Opt. **46,** 4228 (2007).
13. E. Ikonen, P. Toivanen, and A. Lassila, Metrologia **35,** 369 (1998).
14. J. Sheng, L. Zhang, X. Zheng, S. Li, Infrared Laser Eng. **37,** 534 (2008).
15. X. Zheng, H. Wu, J. Zhang, Y. Liu, W. Zhou, L. Wang, and Y. Qiao, Chin. Sci. Bull. **45,** 2009 (2000).
16. J. Li, X. Zheng, Y. Li, W. Zhang, and P. Zhou, Acta Phys. Sin. **58,** 6273 (2009).
17. J. B. Fowler, R. Durvasula, and A. Parr, Metrologia **35,** 497 (1998).
18. J. T. Woodward, A. W. Smith, C. A. Jenkins, C. Lin, S. W. Brown, and K. R. Lykke, Metrologia **46,** S277 (2009).
19. A. Berjón, B. Torres, C. Toledano, T. Podvin, L. Blarel, N. Prats, P. Goloub, and V. Cachorro, J. Aerosol Sci. **59,** 1 (2013).
20. G. Thuillier, L. Floyd, T. N. Woods, R. Cebula, E. Hilsenrath, M. Herse, and D. Labs, in *Solar Variability and Its Effects on Climate.* J. M. Pap, P. Fox, C. Frohlich, H. S. Hudson, J. Kuhn, J. McCormack, G. North, W. Sprigg and S. T. Wu, (eds.) (American Geophysical Union, 2004) pp. 171.